Published in final edited form as:
J Nucl Med. 2005 May ; 46(5): 807–815.

Structural Requirements For In Vivo Detection of Cell Death with ^{99m}Tc-Annexin V

Jonathan F Tait, MD, PhD[1,2,3], **Christina Smith, BS**[1], and **Francis G Blankenberg, MD**[4]

[1]*Departments of Laboratory Medicine;* [2]*Medicine (Medical Genetics); and* [3]*Pathology, University of Washington, Seattle, WA 98195;* [4]*Department of Radiology, Stanford University, Palo Alto, CA 94305*

Abstract

^{99m}Tc-annexin V is used to image cell death in vivo via high-affinity binding to exposed phosphatidylserine. We investigated how changes in membrane binding affinity, molecular charge, and method of labeling affected its biodistribution in normal mice and its uptake in apoptotic tissues.

Methods: An endogenous Tc chelation site (Ala-Gly-Gly-Cys-Gly-His) was added to the N-terminus of annexin V to create annexin V-128. The membrane binding affinity of annexin V-128 was then progressively reduced by one to four mutations in calcium binding sites. In addition, mutations were made in other residues that altered molecular charge without altering membrane binding affinity. All mutant proteins were labeled with ^{99m}Tc at the same N-terminal endogenous chelation site. Wild-type annexin V was also labeled with ^{99m}Tc after derivatization with HYNIC (hydrazinonicotinamide). Radiolabeled proteins were tested for biodistribution in normal mice and in mice treated to induce apoptosis of the liver.

Results: Comparison of Tc-annexin V-128 with Tc-HYNIC-annexin V showed that the protein labeled at the endogenous chelation site had the same or higher uptake in apoptotic tissues, while showing 88% lower renal uptake at 60 min after injection. The blood clearance of annexin V was unaffected by changes in either the membrane binding affinity or the molecular charge. Kidney uptake was unaffected by changes in binding affinity. In marked contrast, uptake in normal liver and spleen decreased markedly as affinity decreased. The same pattern was observed in animals treated with cycloheximide to induce apoptosis. Control experiments with charge mutants showed that the effects seen with the affinity mutants were not due to the concomitant change in molecular charge that occurs in these mutants.

Conclusion: 1) All four domains of annexin V are required for optimal uptake in apoptotic tissues; molecules with only one or two active domains are unlikely to be suitable for imaging of cell death in vivo. 2) Uptake in normal liver and spleen is specific (dependent on phosphatidylserine-binding affinity), whereas renal uptake is non-specific. 3) Tc-annexin V-128 detects cell death as well as Tc-HYNIC-annexin V, while showing 88% less renal retention of radioactivity due to much more rapid urinary excretion of radioactivity.

Keywords

annexin V; apoptosis; biodistribution; mutagenesis (site-specific); phosphatidylserine

Address for correspondence: Dr. Jonathan Tait, Department of Laboratory Medicine, University of Washington, Box 357110, Seattle, WA 98195-7110, Telephone: (206)598-6131, Fax: (206)598-6189, Email: tait@u.washington.edu.

Support: USPHS (NIH grants CA-102348 and EB-000898)

INTRODUCTION

Apoptosis is important in normal physiology and numerous disease states. We have developed annexin V as a means to image cell death in vivo *(1,2)*. This is based on the protein's high affinity for PS (phosphatidylserine) exposed on the extracellular face of cell membranes *(3)*, which occurs when cells undergo apoptosis *(4)*. Annexin V contains four similar domains of 70–80 amino acids arranged in a compact water-soluble structure *(5)*. High-affinity membrane binding depends on multiple calcium binding sites present in all four domains of the molecule *(6)*. Clinical applications for annexin V imaging are being developed in oncology *(7)*, organ transplantation *(8)*, and cardiovascular disease *(9)*.

Although ^{99m}Tc-HYNIC-annexin V has been succesfully used in many studies, it has certain limitations, most notably its very high uptake in the kidney, which results in high radiation dose and may limit imaging in the abdomen *(10)*. Alternative approaches for radiolabeling annexin V with technetium have been described *(11–14)*. Annexin V has also been labeled with F-18 for PET imaging *(15)*. While there is some variation in biodistribution and metabolism of these different radiolabeled annexins, many properties of the protein are the same regardless of the method of labeling. Initial blood clearance is relatively rapid *(11,16,17)*. Organ uptake is almost always highest in the kidney, followed by the liver; there is moderate uptake in spleen, lung, and bowel; uptake is very low in brain, heart, and skeletal muscle. Recently, novel approaches based on modifications of the protein itself have also been described. There has been a report of a single-domain "mini-annexin" that may be useful for imaging *(18)*. Annexin V has also been modified with polyethylene glycol to prolong its circulation time and thereby improve its availability over extended periods for uptake by tumors *(19)*.

As part of an effort to develop improved annexin V-based imaging agents, we wanted to address several questions. First, why do some organs have much higher uptake of annexin V than others? Second, what structural features of annexin V control uptake in both normal and apoptotic tissues? Third, how much loss of membrane binding affinity can be tolerated before annexin V loses its ability to localize in apoptotic tissues? To address these questions, we prepared a series of site-directed mutants of annexin V that alter properties such as charge and membrane binding affinity. We took advantage of the method we previously developed for Tc labeling of annexin V via an N–terminal endogenous chelation site consisting of the amino acid sequence Ala-Gly-Gly-Cys-Gly-His *(12)*. All structural mutants of annexin V contained the same sequence in 1:1 stoichiometry, and therefore the site of Tc labeling was exactly the same for all mutant proteins. Thus, any differences observed could be attributed to the specific mutations introduced rather than differences in the site or degree of labeling. We show that the new annexin V-128 recombinant protein has substantially improved biodistribution properties compared to HYNIC-derivatized annexin V. We also show that alterations in membrane binding affinity change biodistribution in normal animals and target uptake in an animal model of apoptosis. These results provide guidance in the development of improved annexin V-based apoptosis imaging agents radiolabeled with either Tc-99m or positron emitters, as well as annexin V-based agents used for fluorescence or magnetic resonance imaging.

MATERIALS AND METHODS

Preparation and Tc Labeling of Mutant Proteins

Recombinant human annexin V-128 and derivative mutant proteins were prepared and purified as described *(6)*. In preparation for technetium labeling, protein (0.6 mg) was diluted with PBS (phosphate-buffered saline, containing 10 mM sodium phosphate pH 7.4, 140 mM NaCl) to a final volume of 0.2 ml and reduced with 1 mM dithiothreitol at 37°C for 15 min under anaerobic conditions. The protein was applied to a Sephadex G-25 column (NAP-5; Pharmacia,

Piscataway, NJ), which had been pre-equilibrated with deoxygenated buffer (20 mM trisodium citrate, pH 5.4, 100 mM NaCl), and the breakthrough (0.2 ml) was discarded. Elution was performed with the same buffer; the first 0.5 ml of eluate was discarded, and the subsequent 0.5 ml, containing the protein, was collected in argon-flushed glass vials. Aliquots of 0.1 ml (containing 0.1 mg protein, 0.59 mg trisodium citrate, and 0.58 mg NaCl) were stored frozen at −20°C in glass vials with teflon-sealed screw caps. Tin reagent was prepared as described *(12)*. Each vial of lyophilized reagent contained 5 mg of sodium glucoheptonate, 0.128 mg $SnCl_2.2H_2O$, and 0.128 mg of sodium gentisate. Just prior to use, the vial was reconstituted with 0.2 ml of deoxygenated water.

^{99m}Tc-annexin V-128 was prepared as follows. $^{99m}TcO_4$ (5–10 mCi in 0.1 ml of 0.9% NaCl) was added to a polypropylene microfuge tube, followed by 0.005 ml of tin reagent and 0.05 ml (0.05 mg) of reduced protein. After a 60-min anaerobic incubation at 37°C, the reaction mixture was brought to a volume of 0.4 ml with PBS pH 7.4 and applied to a Sephadex G-25 column (Pharmacia NAP-5) equilibrated and eluted with PBS pH 7.4. The labeled protein was collected in a volume of 1.4 ml (0.4 ml of breakthrough and the first 1.0 ml of eluate). Percent incorporation of technetium determined by ITLC was routinely 85–97%, corresponding to a specific activity of about 100 mCi/mg. The labeling reaction can also be performed at room temperature for 20–30 min with minimal loss of labeling efficiency *(12)*. A dose of 0.05 to 0.2 mCi of tracer (0.1 to 0.2 ml, 0.05 to 0.1 mg protein/kg body weight) was injected via tail vein for all animal studies. ^{99m}Tc-HYNIC-annexin V was prepared and labeled with the tin-tricine method as previously described *(1)*.

Membrane Binding Affinity Measurement by Quantitative Calcium Titration

The affinity of labeled protein for RBC (red blood cells) with exposed PS was determined by the calcium titration assay previously described for fluorescently labeled annexin V *(20)*. Annexin V-128 was labeled with ^{99m}Tc as described above and diluted to a working concentration of 200 nM in 50 mM HEPES-sodium, pH 7.4, 100 mM NaCl, 3 mM NaN_3, 5 mg/ml BSA (bovine serum albumin). The final concentration of ^{99m}Tc-annexin V-128 in the assay was 1 nM, RBC were added at 1×10^8 per ml and calcium was varied from 0 to 5 mM, in an assay buffer containing 50 mM HEPES-sodium, pH 7.4, 100 mM NaCl, 3 mM NaN_3, with 1 mg/ml BSA as carrier protein. After an 8-min incubation at room temperature, cells were pelleted by centrifugation, resuspended in 1 ml of assay buffer containing the same concentration of calcium used in the binding step, and centrifuged again. The supernatant was removed and the ^{99m}Tc-annexin V-128 bound to the RBC was released with 0.7 ml of assay buffer containing 5 mM EDTA. The RBC were pelleted by centrifugation and the amount of ^{99m}Tc-annexin V-128 bound to the RBC at each calcium concentration was determined by counting an aliquot (0.3 – 0.6 ml) of the supernatant on a gamma counter (RIASTAR Jr, Hewlett Packard). Calcium titration curves were analyzed to determine the binding affinity as described *(20)*; results are expressed as a pK value, which is the logarithm of the equilibrium constant for protein-membrane-calcium binding.

TUNEL Assay

Livers from normal and cycloheximide-treated mice were evaluated for the presence of apoptotic nuclei in formalin-fixed, paraffin-embedded tissue sections with a fluorescent TUNEL (terminal deoxyribonucleotidyl transferase-mediated deoxyuridine nick-end labelling) assay kit following the manufacturer's directions (Oncogene Research Products Fluorescein-FragEL^{Tm} kit, Calbiochem-Novabiochem Corp, San Diego, CA). The number of apoptotic nuclei was determined from 60 fields per slide, containing an average of 36 nuclei per field, examined under 60x magnification.

Blood Clearance and Biodistribution Studies in Normal and Treated Mice

All mice used were adults (6 to 8 weeks old) of the Balb/c strain obtained from the breeding facility of the Department of Comparative Medicine, Stanford University. Hepatic apoptosis was induced by intraperitoneal injection of cycloheximide *(21)* at a dose of 50 mg/kg dissolved in 0.5 ml of PBS. All animals were anesthetized with a cocktail of ketamine (100 mg/kg intraperitoneal) (Fort Dodge, Iowa) and xylazine (10 mg/kg, intraperitoneal) (Butler, Columbus, Ohio) prior to clearance, biodistribution, and imaging studies. Blood clearance studies were performed by serial retro-orbital blood samples obtained after tail vein injection of tracer. Biodistribution assay was performed immediately after sacrifice. Tissue and organ samples were analyzed with a scintillation well counter along with four samples of standard activity (1/100 of injected dose) at an energy level of 140 keV with an energy window of ± 20 keV. Results are expressed as the average of the percentage of injected dose (ID) or percent ID per gram (g) of tissue (% ID/g) ± one standard deviation of the mean.

Dynamic Imaging

Dynamic planar images of tracer activity were obtained using the ASPECT dedicated small animal imaging SPECT gamma camera (Gamma Medical Instruments; Los Angeles, CA) using a 128 × 128 matrix and a high resolution high sensitivity parallel hole collimator. Sedated animals were placed in the anterior supine position and planar whole-body images were collected starting immediately after injection of tracer via tail vein (animals received the same dose of tracer used for static biodistribution studies); serial one-minute images were obtained for 35 minutes, and serial three-minute images for another 60 minutes. Region of interest (ROI) image analyses were performed on planar images using commercially available software (Mirage™ Software, version 5.3, Segami Corporation, Columbia, MD). The results of the dynamic image analysis for the activity of each region of interest expressed as counts/pixel are reported as the percentage of whole body activity also expressed as counts/pixel.

RESULTS

Characterization of ^{99m}Tc-Annexin V-128

All mutant proteins were built on the base structure of annexin V-128 *(6)*. This protein has essentially the same structure as wild-type human annexin V, except for an N-terminal extension of Ala-Gly-Gly-Cys-Gly-His to provide a site for Tc chelation and a Cys316Ser point mutation. Figure 1 shows a calcium titration curve performed with ^{99m}Tc-annexin V-128 and RBC with exposed PS. The curve is identical to that previously obtained with fluorescently labeled annexin V-128. The pK value for binding of ^{99m}Tc-annexin V-128 to RBC is 30.8 ± 1.0 (mean ± SD, n = 3), identical to that previously reported for both for wild-type annexin V and for annexin V-128 labeled with fluorescein *(6,20)*. Thus, Tc labeling at the N-terminus does not alter binding affinity, consistent with our earlier work with the annexin V-117 protein *(12)*, which has a nearly identical structure.

Comparison of HYNIC-Annexin V and Annexin V-128

In order to verify that ^{99m}Tc-annexin V-128 was suitable for detection of cell death, it was compared with ^{99m}Tc-HYNIC-annexin V in normal mice. As seen in Table 1, the biodistribution of the two proteins was similar overall, with a few exceptions. The most striking exception was the kidney: ^{99m}Tc-annexin V-128 showed 88% less renal uptake than ^{99m}Tc-HYNIC-annexin V. Liver and spleen uptake was also somewhat lower for ^{99m}Tc-annexin V-128, possibly reflecting less aggregated material. Small bowel was the only organ showing higher uptake of ^{99m}Tc-annexin V-128 (3.9% of ID) compared to ^{99m}Tc-HYNIC-annexin V (1.6% of ID). However, this was greatly outweighed by lower overall abdominal uptake of ^{99m}Tc-annexin V-128 (17% of ID, versus 60% of ID for ^{99m}Tc-HYNIC-annexin V).

When mice were treated with cycloheximide to induce apoptosis, liver and spleen showed a several-fold increase in uptake of ^{99m}Tc-annexin V-128 (Fig. 2A). We also verified that uptake of ^{99m}Tc-annexin V-128 was consistent with an independent measure of apoptosis. As shown in Figure 2B, in vivo uptake of ^{99m}Tc-annexin V-128 in the liver correlated closely with histologic analysis of the degree of apoptosis as judged by the TUNEL assay.

Dynamic Imaging with HYNIC-Annexin V and Annexin V-128

The reason for the striking difference in renal uptake of ^{99m}Tc-annexin V-128 compared to ^{99m}Tc-HYNIC-annexin V was further explored via dynamic imaging studies (Fig. 3). Renal uptake of each protein is comparable up to about 15 min after injection. After that time, there is a progressive decline in renal radioactivity for the ^{99m}Tc-annexin V-128 protein, accompanied by a corresponding increase in radioactivity in the bladder. In contrast, for ^{99m}Tc-HYNIC-annexin V, radioactivity in the kidney stays roughly constant, and there is minimal bladder excretion during this time. These results were confirmed by static biodistribution measurements performed at 15 min after injection, which confirmed that the renal uptake of ^{99m}Tc-annexin V-128 and ^{99m}Tc-HYNIC-annexin V was comparable at that time (data not shown).

Characterization of Charge and Affinity Mutants

To determine how PS binding affinity and molecular charge affect biodistribution and target uptake of annexin V, a series of mutants were prepared (Fig. 4; Table 2). The PS binding affinity of annexin V can be reduced in a stepwise fashion by making point mutations in aspartate or glutamate residues contributing to the AB-helix calcium binding sites present once in each of the four domains *(6)*. These mutants span a very broad range of membrane binding affinity (as summarized on a logarithmic scale by the pK affinity value) but they all have essentially the same molecular mass as the parent protein, since each mutation changes molecular mass by only one dalton. Since mutations in the AB-helix calcium binding sites also alter molecular charge by converting a negatively charged residue to a neutral residue, a second set of mutant proteins was prepared with unaltered affinity but altered molecular charge as control proteins to evaluate the specificity of changes observed with the affinity mutants. Some of these mutant proteins have been previously reported *(6)*, and others were developed specifically for this study.

Blood Clearance of Affinity Mutants

The blood clearance of ^{99m}Tc-annexin V-128 and selected affinity mutants was measured in mice (Fig. 5). All proteins showed the same rapid clearance kinetics, with only 4% remaining in blood at 60 min. These clearance curves are essentially the same as those previously reported for unlabeled annexin V *(16)*, ^{125}I-annexin V and ^{123}I-annexin V *(11,17)* and HYNIC-annexin V *(22)*. Thus, changes in PS-binding affinity do not alter the kinetics of blood clearance of annexin V. Similarly, changes in molecular charge did not alter blood clearance (data not shown).

Uptake in Apoptotic Organs

To determine the impact of affinity changes on uptake in apoptotic organs, we tested the series of affinity mutants in mice treated with cycloheximide to induce apoptosis of the liver and spleen (Fig. 6A). There was a clear dose-response relationship between the number of mutations and the reduction in organ uptake in the liver and spleen. A single mutation decreased uptake by 50–60%, and the presence of two or more mutations reduced uptake by 80–90%. However, the specific location of the mutation in the molecule (Fig. 4) did not influence the results: single-site mutants in domains 1 and 4 were equivalent, double mutants in domains 1 +4 and domains 2+3 were equivalent, and triple mutants in domains 1+2+4 and domains 2+3

+4 were equivalent. Thus, the dominant factor determining uptake in apoptotic tissue is the total number of active domains rather than the specific site of the mutation(s); in other words, membrane binding sites in each of the four domains are equivalent in their influence on target uptake in vivo.

As a control, we also determined the effect of affinity mutations on the uptake in normal liver and spleen (Fig. 6B). Somewhat unexpectedly, a similar pattern was observed: organ uptake was progressively reduced by increasing number of mutations. To verify that this effect on normal organ uptake was not an artifact of concomitant changes in molecular charge that occur in the affinity mutants, a second series of mutant proteins was tested that altered charge without affecting PS-binding affinity (Fig. 7). Charge differences from −2 to +2 relative to wild-type protein did not affect the uptake in normal liver or spleen, indicating that the effects observed in Figure 8 were due to affinity changes rather than changes in charge per se.

In view of the results obtained with normal liver and spleen, we carried out a more extensive evaluation of the effect of PS-binding affinity on biodistribution in normal animals (Fig. 8). Biodistribution was measured with triple and quadruple mutant proteins (i.e., annexin V-137, -143, and –145). Results for individual organs fell into three groups. For the spleen, liver, and lung, 75–85% of uptake was eliminated by eliminating the PS-binding activity of annexin V. For the stomach, small bowel, and heart, about 40–50% of uptake was lost in the mutants compared to the wild-type protein. For the kidney and large bowel, uptake was unaffected by changes in affinity.

DISCUSSION

Characterization of ^{99m}Tc-Annexin V-128 and Comparison With ^{99m}Tc-HYNIC-Annexin V

We have recently developed a novel form of annexin V with an endogenous Tc chelation site, termed annexin V-128 *(6)*, that has significant advantages over ^{99m}Tc-HYNIC-annexin V. There is a striking difference in the renal handling of Tc-labeled annexin V depending on the method of labeling. Initial renal uptake is the same, but subsequent urinary excretion of ^{99m}Tc is far more rapid for the ^{99m}Tc-annexin V-128 derivative compared to the ^{99m}Tc-HYNIC-annexin V derivative. The most likely explanation is as follows. Both proteins are filtered equally at the glomerulus, and both are taken up in the proximal tubules by relatively non-specific uptake systems designed to capture low-molecular-weight proteins *(23)*. Endocytosed proteins are then delivered to the lysosome and degraded by proteases to oligopeptides or amino acids. However, the end products differ greatly in their retention in the kidney. The end product of the degradation of ^{99m}Tc-HYNIC-annexin V is probably the lysine adduct of ^{99m}Tc-HYNIC complexed to tricine, which has a high degree of retention in lysosomes *(24,25)*. The end product of the metabolism of ^{99m}Tc-annexin V-128 is not known, but may consist either of a small oligopeptide or possibly pertechnetate alone. In any event, the radioactive end product is much more rapidly excreted from the kidney. Although we did not study metabolism of ^{99m}Tc-annexin V-128 in other organs, it seems unlikely that the rapid degradation seen in the kidney would also occur in apoptotic tissues because apoptotic bodies will have lost the multiple systems required for endocytosis, intracellular transport, and degradation of proteins bound to the cell surface. Thus, annexin V is likely to remain intact when bound to the surface of dead cells or their fragments.

The improvements in biodistribution achieved with annexin V-128 were obtained without any compromise in its ability to detect apoptosis in vivo, as shown by Figure 2. This protein also has significant advantages for manufacturing compared to HYNIC-annexin V: the end-product of recombinant protein production is ready to be labeled directly with ^{99m}Tc, and does not need to undergo further chemical derivatization, purification, and characterization. The single labeling site at the N-terminus is uniform and well-characterized; this region of the protein is

on the opposite side of the molecule from the membrane binding region *(5)*. In contrast, it can be difficult to obtain a reproducible preparation of chemically modified annexin V when amine-directed reagents are used; inevitably, the product is heterogeneous with respect to sites and stoichiometry of labeling. The Tc labeling procedure is comparable in simplicity to that used with HYNIC-annexin: one simply mixes pertechnetate, tin reagent and protein and incubates for 20–60 min at 22° or 37° (this study; *(12)*). Overall, ^{99m}Tc-annexin V-128 is an attractive candidate to replace ^{99m}Tc-HYNIC-annexin V in many applications.

Factors Regulating Normal Organ Uptake of Annexin V

This study shows that uptake of annexin V in normal organs is differentially regulated. In some organs, such as liver, spleen, and lung, uptake is an inherent property of the protein, and is primarily dependent on the PS-binding affinity of the molecule. In other organs, such as kidney and large bowel, uptake is relatively non-specific, and is not regulated by the PS-binding affinity of the molecule. Some organs, such as stomach, small bowel, and heart, are in between, with about half their normal uptake being PS-specific. Control experiments showed that these effects were not simply due to charge changes introduced by the point mutations used to reduce binding affinity. Similarly, the observed effects were not due to molecular weight changes, since the point mutations change the protein's molecular mass by only one to four daltons *(6)*.

There are several possible explanations for the differential effects of PSbinding affinity on organ uptake. It is possible that the results reflect different levels of physiologic apoptosis in different organs. It is also possible that annexin V is binding to apoptotic cells or cell debris that is in the process of being engulfed by phagocytic cells in the liver, spleen, and lung. It is also possible that annexin V is binding to non-PS substances in some normal organs – for example, annexin V is known to bind to anionic polysaccharides such as heparan sulfate under some conditions *(26)*. Finally, annexin V could be taken up by an organ-specific endocytic mechanism that is somehow dependent on its membrane binding affinity. In any event, the results of this study show that factors governing the biodistribution of annexin V are complex, and are not simply a function of non-specific factors such as molecular size, charge or vascular permeability.

Affinity Requirements for Annexin V Uptake in Apoptotic Tissues

Our results indicate clearly that all four domains of annexin V are needed for maximum uptake in apoptotic organs in vivo. Although previous work had suggested that most of the in vitro binding affinity of annexin V was concentrated in the first domain *(27)*, our recent work with improved assay methods showed clearly that all four domains contribute equally to in vitro binding affinity *(6)*. The results in this paper now extend these observations to organ uptake in vivo. It is clear that organ uptake is a function only of the total number of active domains, and is not affected by the specific domain(s) that have been inactivated by mutation. For example, single-site mutants in domains 1 and 4 behaved equivalently, as did double mutants in domains 1+4 versus domains 2+3; there was no difference between mutants containing different combinations of individual mutations, provided they contained the same total number of mutations.

This study also confirms the value of our recently developed methods for measuring the affinity of annexin V for membranes in vitro *(20)*. These methods rely on quantitative calcium titration at low ratios of protein to membrane, which are probably most relevant to the in vivo situation. Although we have previously used this method with fluorescently labeled protein, the results of Figure 1 show that the method works equally well for cell binding assays performed with radioactively labeled protein. We believe that these methods are the best overall means of measuring the membrane binding affinity of modified annexins and will provide the best

overall prediction of in vivo uptake. The logarithm of the binding constant (pK value) quantitatively predicts in vivo uptake: pK values 25% below wild-type are associated with significant loss of in vivo uptake, and pK values below 50% of wild-type are associated with complete loss of in vivo uptake (Table 2 and Figure 6A). It should be noted that the pK value is logarithmic; a decrease of one pK unit corresponds to a tenfold reduction in the equilbrium constant.

CONCLUSION

There are several implications of this work for the further development of annexin V as an imaging agent for cell death in vivo. First, it appears that annexin V derivatives based on a single active domain *(18)*, instead of the full four domains of the native protein, will probably lack the binding affinity required to provide effective target localization in vivo. Second, since the binding surface of annexin V encompasses contributions from all four domains *(6,20)*, caution should be exercised in amine-directed labeling strategies that affect multiple residues on the same protein molecule, since there are multiple lysine residues present on or near the membrane-binding face of the molecule *(5)*. However, modest changes in molecular charge per se, as can typically occur with modification of single lysine residues and/or the amino terminus, are unlikely to alter the clearance, biodistribution or metabolism of the molecule. Finally, the use of the N-terminal endogenous Tc chelation sequence appears to have major advantages over the HYNIC chelator with regard to renal retention of ^{99m}Tc, with attendant decreased abdominal background and renal radiation dose.

Acknowledgements

Supported by NIH grants CA-102348 and EB-000898. We thank Donald Gibson for preparing experimental materials, and the Theseus Imaging Corporation and Dr. Jean-Luc Vanderheyden for the NAS 2020 HYNIC-annexin V and tin-tricine kits.

References

1. Blankenberg FG, Katsikis PD, Tait JF, et al. In vivo detection and imaging of phosphatidylserine expression during programmed cell death. Proc Natl Acad Sci U S A 1998;95:6349–6354. [PubMed: 9600968]
2. Blankenberg FG, Katsikis PD, Tait JF, et al. Imaging of apoptosis (programmed cell death) with 99mTc annexin V. J Nucl Med 1999;40:184–191. [PubMed: 9935075]
3. Thiagarajan P, Tait JF. Binding of annexin V/placental anticoagulant protein I to platelets. Evidence for phosphatidylserine exposure in the procoagulant response of activated platelets. J Biol Chem 1990;265:17420–17423. [PubMed: 2145274]
4. Fadok VA, Voelker DR, Campbell PA, Cohen JJ, Bratton DL, Henson PM. Exposure of phosphatidylserine on the surface of apoptotic lymphocytes triggers specific recognition and removal by macrophages. J Immunol 1992;148:2207–2216. [PubMed: 1545126]
5. Huber R, Berendes R, Burger A, et al. Crystal and molecular structure of human annexin V after refinement. Implications for structure, membrane binding and ion channel formation of the annexin family of proteins. J Mol Biol 1992;223:683–704. [PubMed: 1311770]
6. Jin M, Smith C, Hsieh HY, Gibson DF, Tait JF. Essential role of B-helix calcium binding sites in annexin V-membrane binding. J Biol Chem 2004;279:40351–40357. [PubMed: 15280367]
7. Belhocine T, Steinmetz N, Hustinx R, et al. Increased uptake of the apoptosis-imaging agent (99m)Tc recombinant human annexin V in human tumors after one course of chemotherapy as a predictor of tumor response and patient prognosis. Clin Cancer Res 2002;8:2766–2774. [PubMed: 12231515]
8. Narula J, Acio ER, Narula N, et al. Annexin-V imaging for noninvasive detection of cardiac allograft rejection. Nat Med 2001;7:1347–1352. [PubMed: 11726976]
9. Hofstra L, Liem IH, Dumont EA, et al. Visualisation of cell death in vivo in patients with acute myocardial infarction. Lancet 2000;356:209–212. [PubMed: 10963199]

10. Kemerink GJ, Liu X, Kieffer D, et al. Safety, biodistribution, and dosimetry of 99mTc-HYNIC-annexin V, a novel human recombinant annexin V for human application. J Nucl Med 2003;44:947–952. [PubMed: 12791824]
11. Stratton JR, Dewhurst TA, Kasina S, et al. Selective uptake of radiolabeled annexin V on acute porcine left atrial thrombi. Circulation 1995;92:3113–3121. [PubMed: 7586283]
12. Tait JF, Brown DS, Gibson DF, Blankenberg FG, Strauss HW. Development and characterization of annexin V mutants with endogenous chelation sites for (99m)Tc. Bioconjug Chem 2000;11:918–925. [PubMed: 11087342]
13. Kemerink GJ, Boersma HH, Thimister PW, et al. Biodistribution and dosimetry of 99mTc-BTAP-annexin-V in humans. Eur J Nucl Med 2001;28:1373–1378. [PubMed: 11585297]
14. Tait JF, Smith C, Gibson DF. Development of annexin V mutants suitable for labeling with Tc(I)-carbonyl complex. Bioconjugate Chem 2002;13:1119–1123.
15. Zijlstra S, Gunawan J, Burchert W. Synthesis and evaluation of a 18F-labelled recombinant annexin-V derivative, for identification and quantification of apoptotic cells with PET. Appl Radiat Isot 2003;58:201–207. [PubMed: 12573319]
16. Romisch J, Seiffge D, Reiner G, Paques EP, Heimburger N. In-vivo antithrombotic potency of placenta protein 4 (annexin V). Thromb Res 1991;61:93–104. [PubMed: 1826976]
17. Tait JF, Cerqueira MD, Dewhurst TA, Fujikawa K, Ritchie JL, Stratton JR. Evaluation of annexin V as a platelet-directed thrombus targeting agent. Thromb Res 1994;75:491–501. [PubMed: 7992250]
18. Blondel A, Vuillemard C, Tavitian B, et al. A new SPECT tracer for improved apoptosis imaging in tumor bearing mice [abstract]. J Nucl Med 2003;44:98P. [PubMed: 12515882]
19. Ke S, Wen X, Wu QP, et al. Imaging taxane-induced tumor apoptosis using PEGylated, 111 In-labeled annexin V. J Nucl Med 2004;45:108–115. [PubMed: 14734682]
20. Tait JF, Gibson DF, Smith C. Measurement of the affinity and cooperativity of annexin V-membrane binding under conditions of low membrane occupancy. Analytical Biochemistry 2004;329:112–119. [PubMed: 15136173]
21. Ledda-Columbano GM, Coni P, Faa G, Manenti G, Columbano A. Rapid induction of apoptosis in rat liver by cycloheximide. Am J Pathol 1992;140:545–549. [PubMed: 1546740]
22. Ohtsuki K, Akashi K, Aoka Y, et al. Technetium-99m HYNIC-annexin V: a potential radiopharmaceutical for the in-vivo detection of apoptosis. Eur J Nucl Med 1999;26:1251–1258. [PubMed: 10541822]
23. Verroust PJ, Birn H, Nielsen R, Kozyraki R, Christensen EI. The tandem endocytic receptors megalin and cubilin are important proteins in renal pathology. Kidney Int 2002;62:745–756. [PubMed: 12164855]
24. Ono M, Arano Y, Uehara T, et al. Intracellular metabolic fate of radioactivity after injection of technetium-99m-labeled hydrazino nicotinamide derivatized proteins. Bioconjug Chem 1999;10:386–394. [PubMed: 10346868]
25. Ono M, Arano Y, Mukai T, et al. Control of radioactivity pharmacokinetics of 99mTc-HYNIC-labeled polypeptides derivatized with ternary ligand complexes. Bioconjug Chem 2002;13:491–501. [PubMed: 12009938]
26. Capila I, Hernaiz MJ, Mo YD, et al. Annexin V--heparin oligosaccharide complex suggests heparan sulfate-- mediated assembly on cell surfaces. Structure (Camb) 2001;9:57–64. [PubMed: 11342135]
27. Montaville P, Neumann J-M, Russo-Marie F, Ochsenbein F, Sanson A. A new consensus sequence for phosphatidylserine recognition by annexins. J Biol Chem 2002;277:24684–24693. [PubMed: 11948176]

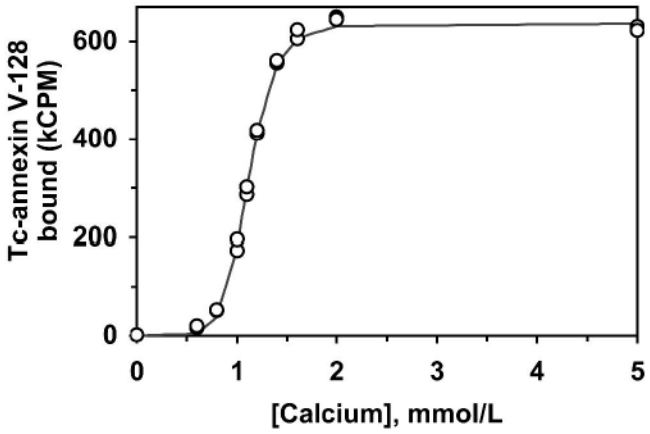

FIGURE 1.

Calcium titration of ^{99m}Tc-annexin V-128 binding to RBC with exposed PS. The line is the fitted function used to determine the EC_{50} and Hill coefficient values, from which the logarithm of the binding constant (pK value) is calculated *(20)*.

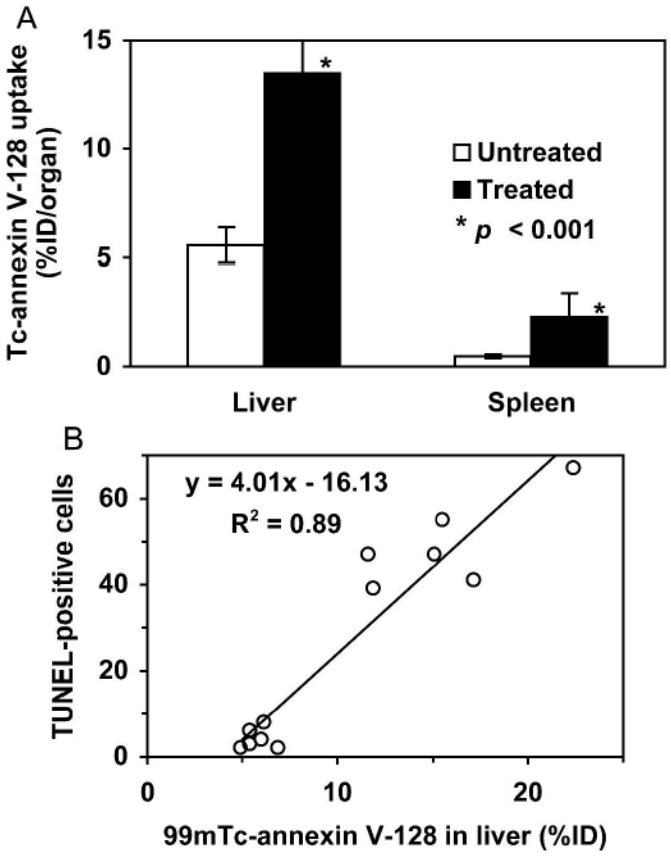

FIGURE 2.

(A) Uptake of ^{99m}Tc-annexin V-128 in liver and spleen of mice treated with cycloheximide. Groups of six mice were either untreated or treated with cycloheximide (50 mg/kg intraperitoneal). Two hours later, ^{99m}Tc-annexin V-128 was injected via the tail vein, and organs were harvested 60 min after the injection. Significance of the difference between treated and untreated animals was assessed by a two-tailed t-test assuming unequal variances; error bars indicate SD. (B) Correlation between TUNEL positivity and ^{99m}Tc-annexin V-128 uptake in liver for treated and untreated mice (six in each group).

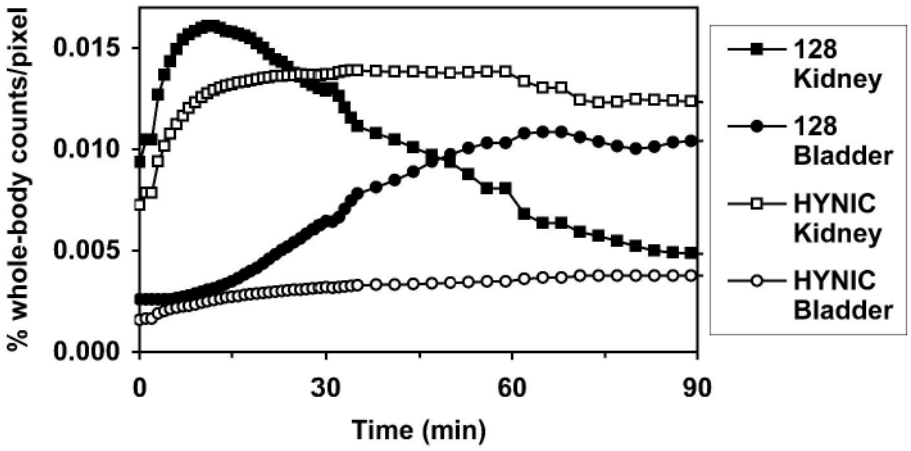

FIGURE 3.

Serial dynamic imaging of kidney and bladder uptake of ^{99m}Tc-annexin V-128 and ^{99m}Tc-HYNIC-annexin V. Each curve is the mean of four animals; the coefficient of variation at each point is approximately 20%.

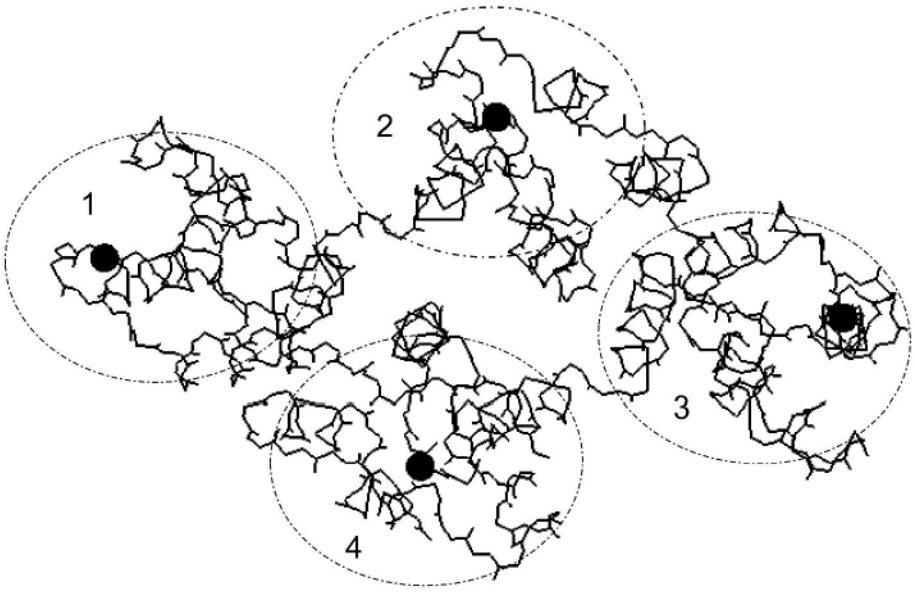

FIGURE 4.

Schematic view of the three-dimensional structure of annexin V-128. The view is downward onto the membrane binding face of the protein. The four domains of the protein are numbered, and their approximate locations are indicated by the ellipses. Black spheres indicate the approximate locations of calcium ions bound to the AB-helix calcium binding sites that have been mutated in this study. The polypeptide backbone is shown as a continuous black line. The location of the N-terminal technetium chelation site can not be seen in this projection because it is on the opposite face of the molecule, beneath the plane of the page. (Structure is based on preliminary coordinates provided by Dr. Barbara Seaton (personal communication.)

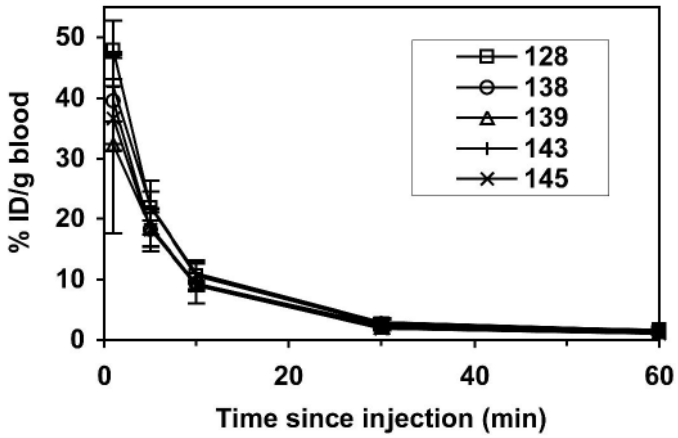

FIGURE 5.
Blood clearance of affinity mutants. Groups of four mice received intravenous injections of Tc-labeled protein at time zero. Results are given as mean ± SD for each mutant.

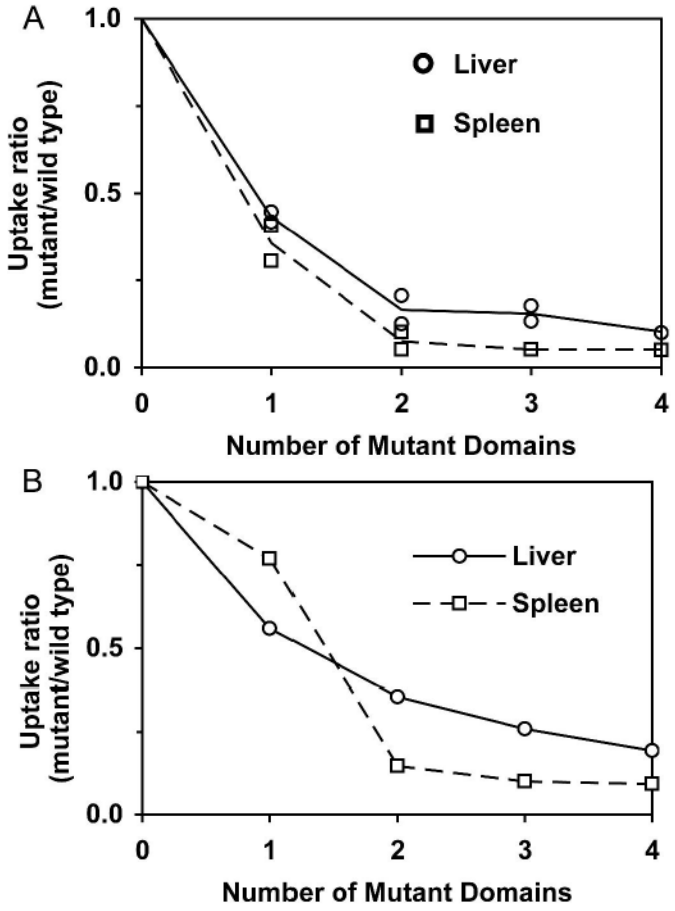

FIGURE 6.

(A) Dose-response relationship between number of affinity-reducing mutations and liver and spleen uptake in mice treated with cycloheximide. Each affinity mutant in Table 2 was tested in groups of 4–5 mice. Mean values are given for liver (○) and spleen (□) uptake, normalized to the uptake observed with wild-type protein. Mutants tested were 128 (wild-type/zero mutations); 131 and 138 (one mutation); 136 and 139 (two mutations); 137 and 143 (three mutations); 145 (four mutations). (B) Dose-response relationship between number of affinity-reducing mutations and liver and spleen uptake in normal mice.

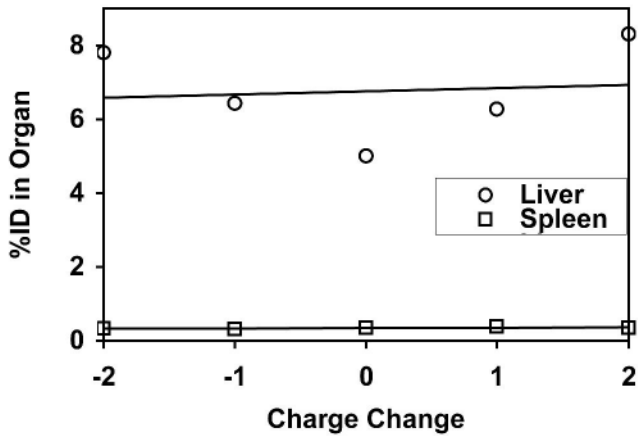

FIGURE 7.

Effect of molecular charge on liver and spleen uptake of Tc-annexin V-128 in normal mice. Each charge mutant in Table 2 was tested in groups of 4–5 mice. Mean values are given for liver (○) and spleen (□) uptake.

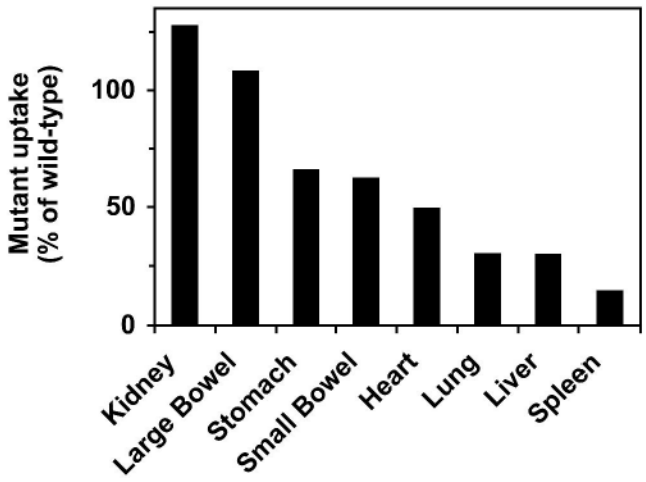

FIGURE 8.

Organ uptake of affinity mutants in normal mice. The triple and quadruple mutants in Table 2 (annexin V-137,-143, and -145) were tested in groups of 4–5 mice for each mutant. Results were averaged for all three mutant proteins and expressed as a percentage of the organ uptake observed with the wild-type protein (annexin V-128).

TABLE 1

Biodistribution of ^{99m} Tc-HYNIC-annexin V and ^{99m}Tc-annexin V-128. Mice were injected with the indicated protein and organs harvested 60 min later. A total of 25 mice were tested with ^{99m}Tc-annexin V-128 and 10 mice with ^{99m}Tc-HYNIC-annexin V. For blood, the %ID was calculated based on an average body mass of 25g and a blood volume of 8% of body mass.

	% ID per organ				% ID per gram			
	Annexin V-128		HYNIC-Annexin V		Annexin V-128		HYNIC-Annexin V	
Organ	Mean	SD	Mean	SD	Mean	SD	Mean	SD
Liver	5.56	0.81	8.07	1.85	4.51	0.61	6.65	1.02
Small Bowel	3.90	0.73	1.58	0.15	2.76	0.42	0.97	0.09
Kidney (one)	3.37	0.51	24.2	2.14	14.2	3.32	114.3	17.1
Large Bowel	0.56	0.27	0.56	0.13	0.79	0.38	0.66	0.07
Lung	0.48	0.08	0.56	0.14	2.11	0.30	2.56	0.68
Spleen	0.46	0.09	0.81	0.16	3.04	0.58	6.52	1.56
Stomach	0.24	0.07	0.35	0.06	1.04	0.23	1.33	0.19
Femur (one)	0.10	0.03	0.14	0.03	0.66	0.18	0.78	0.14
Heart	0.09	0.02	0.18	0.03	0.64	0.12	1.20	0.25
Thymus	0.04	0.01	0.04	0.01	0.33	0.12	0.48	0.11
Blood	1.12	0.22	3.54	0.62	0.56	0.11	1.77	0.31
Muscle					0.39	0.11	0.37	0.08
Fat					0.34	0.39	0.41	0.29

TABLE 2

Summary of affinity and charge mutants. The mutation(s) present are given in single-letter amino acid code. The RBC binding affinity was determined by calcium titration as described *(20)*. Binding affinity of annexin V-137, -143, and -145 was determined by phospholipid vesicle binding assay *(6)* because binding affinity is too weak to measure by RBC binding assay.

Protein Name	Mutation(s)	Domian(s) Affected	Charge Change	Log Binding Affinity (pk)
Annexin V-128	None (wild type)	None	0	30.8
Affinity mutants				
Annexin V-131	D303N	4	1	22.4
Annexin V-138	E72Q	1	1	22.4
Annexin V-136	D144N, E228Q	2,3	2	13.9
Annexin V-139	E72Q, D303N	1,4	2	15.8
Annexin V-137	D144N, E228Q, D303N	2,3,4	3	38% of wt
Annexin V-143	E72Q, D144N, D303N	1,2,4	3	38% of wt
Annexin V-145	E72Q, D144N, E228Q, D303N	1,2,3,4	4	18% of wt
Charge mutants				
Annexin V-177	R18E	1	−2	30.9
Annexin V-178	R6Q	1	−1	32.1
Annexin V-158	E234Q	3	1	31.3
Annexin V-175	E78Q, E234Q	1,3	2	28.8